Molecular Nanomagnets

DOI: 10.1002/anie.201308047

Field-Induced Hysteresis and Quantum Tunneling of the Magnetization in a Mononuclear Manganese(III) Complex**

Julia Vallejo, Alejandro Pascual-Álvarez, Joan Cano, Isabel Castro, Miguel Julve, Francesc Lloret, J. Krzystek, Giovanni De Munno, Donatella Armentano,* Wolfgang Wernsdorfer, Rafael Ruiz-García, and Emilio Pardo**

High-nuclearity complexes of transition-metal ions have been of special interest during the last two decades owing to the possibility of observing slow magnetic relaxation effects at the molecular level.[1] These molecular nanomagnets have potential applications as new high-density magnetic memories and quantum-computing devices in the field of molecular spintronics.[2] The first example of a discrete molecule exhibiting hysteresis and quantum tunneling of the magnetization was the mixed-valent dodecanuclear manganese(III,IV) complex $[Mn_{12}O_{12}(CH_3CO_2)_{16}(H_2O)_4]$.[3] Since then, a plethora of both homo- and heterovalent, manganese-based molecular nanomagnets of varying metal oxidation states (i.e., Mn^{II}, Mn^{III} and/or Mn^{IV}) have been reported, with nuclearities from up to $[Mn^{III}_{84}]$ down to the smaller $[Mn^{III}_2]$ species.[4] However, to our knowledge, there are no examples of mononuclear manganese complexes exhibiting the slow magnetic relaxation effects typical of molecular nanomagnets, referred to as single-ion magnet (SIMs). This is somewhat puzzling, since several SIMs of other highly anisotropic first-row transition metals (i.e., Co^{II} and $Fe^{I/II/III}$) have been recently reported which has rekindled the debate in the field of single-molecular magnetism.[5]

The six-coordinated octahedral high-spin d^4 Mn^{III} ion ($S = 2$) has an orbitally degenerate ^5E_g ground electronic term that is split by the Jahn–Teller effect into $^5A_{1g}$ and $^5B_{1g}$ orbital singlet low-lying states. Owing to the large mixing between them, second-order spin-orbit coupling (SOC) effects are ultimately responsible for the occurrence of a large axial magnetic anisotropy whose sign depends on the ground state, that is, on the nature of the axial tetragonal distortion.[6] For an axially elongated octahedral Mn^{III} environment, negative D values are expected that can potentially lead to a large energy barrier for the magnetization reversal between the two lowest $M_S = \pm 2$ states. To provide this type of geometry and obtain manganese(III)-based SIMs, planar tetradentate chelating ligands with strong donor groups are a well-suited choice.[7]

Herein, we report a complete study on the synthesis, structural characterization, spectroscopic and magnetic properties, and theoretical calculations of $Ph_4P[Mn(opbaCl_2)(py)_2]$ (**1**) [$H_4opbaCl_2 = N,N'$-3,4-dichloro-*o*-phenylenebis(oxamic acid), py = pyridine, and Ph_4P^+ = tetraphenylphosphonium cation]. Complex **1** is the first example of a mononuclear manganese(III) complex exhibiting a field-induced slow magnetic relaxation behavior, thus increasing the number of first-row transition-metal-ion SIMs.

Complex **1** was obtained as well-formed deep brown cubic prisms by slow evaporation of a methanol/pyridine (1:4 v/v) solution of its tetramethylammonium salt in the presence of an excess of Ph_4PCl (see Supporting Information). It crystallizes in the $P2_1/c$ space group of the monoclinic system (Table S1, Supporting Information). The crystal structure of **1** consists of mononuclear manganese(III) complex anions, $[Mn(opbaCl_2)(py)_2]^-$ (Figure 1), which are well separated from each other due to the presence of the bulky tetraphenylphosphonium countercations (Figure S1, Supporting Information).

The manganese atom of **1** has a tetragonally elongated octahedral coordination geometry which is typical of the Jahn–Teller distorted d^4 Mn^{III} ion. The equatorial plane is formed by two amidate nitrogen and two carboxylate oxygen atoms from the $opbaCl_2$ ligand, while the axial positions are occupied by two pyridine nitrogen atoms (Figure 1a). The planar $opbaCl_2$ ligand adopts a tetradentate coordination

[*] J. Vallejo, A. Pascual-Álvarez, Dr. J. Cano, Dr. I. Castro, Prof. Dr. M. Julve, Prof. Dr. F. Lloret, Dr. R. Ruiz-García, Dr. E. Pardo
Departament de Química Inorgànica, Instituto de CienciaMolecular (ICMOL), Universitat de València
46980 Paterna, València (Spain)
E-mail: joan.cano@uv.es
emilio.pardo@uv.es

Dr. J. Krzystek
National High Magnetic Field Laboratory, Florida State University
Tallahassee, FL 32310 (USA)

Prof. Dr. G. De Munno, Dr. D. Armentano
CEMIF.CAL, Dipartimento di Chimica e Tecnologie Chimiche
Università della Calabria
87030, Cosenza (Italy)
E-mail: donatella.armentano@unical.it

Prof. Dr. W. Wernsdorfer
Institut Néel, CNRS, Nanoscience Department
BP 166, 380412 Grenoble Cedex 9 (France)

[**] This work was supported by the MICINN (Spain) (Project CTQ2010-15364), the University of Valencia (Project UV-INV-AE11-38904), the Generalitat Valenciana (Spain) (Projects PROMETEO/20. 09/108, GV/2012/051 and ISIC/2012/002), and the MiUR (Italy) through the Centro di Eccellenza CEMIF.CAL (Grant CLAB01TYEF). J.V. and E.P. thank the MICINN for contracts. HFEPR experiments were performed at the NHMFL, which is funded by the US National Science Foundation through Cooperative Agreement DMR 1157490, the State of Florida, and the DOE. We thank Dr. A. Ozarowski for his EPR simulation program SPIN. E.P. thanks the Ayuntamiento de Valencia for a contract.

Supporting information for this article is available on the WWW under http://dx.doi.org/10.1002/anie.201308047.

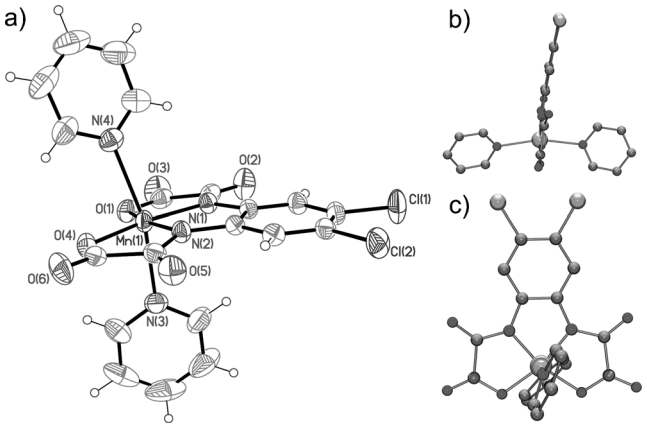

Figure 1. a) ORTEP drawing of the anionic mononuclear manganese(III) unit of **1** (the thermal ellipsoids are set at 50% probability). b) Side and c) top views of the mononuclear manganese(III) unit of **1**.[13]

mode forming three five-membered chelate rings around the manganese(III) ion. This pattern of 5-5-5 fused chelate rings imposes a severe distortion of the equatorial metal environment. Thus, three of the equatorial bond angles at the manganese(III) ion are roughly equal and close to the value of 90° for an ideal octahedron (N(1)-Mn(1)-N(2) 81.63(7)°, N(1)-Mn(1)-O(1) 83.07(6)°, and N(2)-Mn(1)-O(4) 83.40(7)°), while the fourth one, being less constrained, is appreciably larger (O(1)-Mn(1)-O(4) 111.72(6)°). The axial bond angle (N(3)-Mn(1)-N(4) 163.87(6)°) also departs significantly from linearity.

These structural features lead to an overall rhombic (C_{2v}) distortion of the octahedral MnN_4O_2 environment in **1**. The average value of the equatorial Mn–N bond (R(Mn-N_{eq}) = 1.937(2) Å) is somewhat shorter than the equatorial Mn–O one (R(Mn-O_{eq}) = 1.958(2) Å), both of them being shorter than the average axial Mn–N bond length (R(Mn-N_{ax}) = 2.395(2) Å). The resulting axially elongated, trapezoidal bipyramidal geometry of the Mn^{III} ion in **1** may be described by the effective structural rhombicity parameters $\delta_{eq} = [R(\text{Mn-O}_{eq}) - R(\text{Mn-N}_{eq})]/R(\text{Mn-N}_{eq}) = 0.01$ and $\delta_{ax} = [R(\text{Mn-N}_{ax}) - R(\text{Mn-N}_{eq})]/R(\text{Mn-N}_{eq}) = 0.24$.

The anionic mononuclear manganese(III) unit of **1** has, however, a reduced C_1 symmetry because the opbaCl_2 ligand is somewhat bent and the axially coordinated pyridine rings are slightly tilted around the axial vector (Figures 1b and c). The values of the dihedral angle between the 4,5-dichloro-*o*-phenylene fragment and the mean planes of the two oxamate groups are 4.4(1) and 9.3(1)°, while that between the two pyridine rings is 32.1(1)°. This situation is likely explained by the occurrence of weak intermolecular C-Cl···π interactions involving the dichloro-substituted benzene and pyridine rings from neighboring anionic mononuclear Mn^{III} units, together with C-H···O type interactions between the phenyl rings of the Ph_4P^+ ions and the carboxylate oxygen atoms of the oxamate groups from the anionic mononuclear Mn^{III} units (Figures S1 and S2). The shorter intermolecular Mn(1)···Mn(1b) and P(1)···P(1d) separations are 9.401(1) and 6.536(2) Å, respectively [symmetry code: (b) = $-x$, $-y$, $1-z$; (d) = x, $-y+1/2$, $z-1/2$] (Figures S2 and S3).

The direct current (dc) magnetic properties of **1** in the form of the $\chi_M T$ versus T (χ_M being the dc magnetic susceptibility per mononuclear unit) and M versus H/T plots (M being the dc molar magnetization per mononuclear unit and H the applied magnetic dc field) were investigated (Figure S4). The $\chi_M T$ value of 2.99 $cm^3 mol^{-1} K$ at room temperature for **1** is very close to that expected for one high-spin d^4 Mn^{III} ion ($\chi_M T = (N\beta^2 g^2/3k_B)S(S+1) = 3.0\ cm^3 mol^{-1} K$ with $S = 2$ and $g = 2.0$, where N is the Avogadro number, β is the Bohr magneton, and k_B is the Boltzmann constant). Upon cooling, $\chi_M T$ remains almost constant until 40 K and then it decreases abruptly to reach a value of 2.22 $cm^3 mol^{-1} K$ at 2.0 K (Figure S4a), revealing the occurrence of a significant zero-field splitting (zfs). Moreover, the isothermal magnetization curves of **1** in the temperature range of 2–10 K do not superimpose at high H/T values (Figure S4b). Overall, this supports the presence of a significant single-ion magnetic anisotropy of the quintet ground state of the high-spin Mn^{III} ion in **1**, as expected for a tetragonally elongated octahedral geometry.[8]

The experimental magnetic susceptibility and magnetization data of **1** were simultaneously analyzed by using the appropriate spin Hamiltonian for a mononuclear model [Eq. (1)]

$$\boldsymbol{H} = D[\boldsymbol{S}_z^2 + (1/3)S(S+1)] + E(\boldsymbol{S}_x^2 + \boldsymbol{S}_y^2) + \beta H g \boldsymbol{S} \qquad (1)$$

which takes into account both the axial (D) and rhombic (E) magnetic anisotropies of the high-spin d^4 Mn^{III} ion in a rhombically distorted octahedral geometry. The least-squares fit of the experimental data of **1** through the VPMAG program[9] gave $D = -3.271(1)\ cm^{-1}$, $E = -0.105(1)\ cm^{-1}$, and $g = 1.998(1)$ with $F = 1.7 \times 10^{-4}$ (F is the agreement factor defined as $F = \Sigma[(\chi_M T)_{exp} - (\chi_M T)_{calcd}]^2 / \Sigma[(\chi_M T)_{exp}]^2$). The theoretical curves match very well the experimental data in the whole temperature range (solid lines in Figure S4). The values of the best-fit parameters for **1** are similar to those observed in related mononuclear high-spin Mn^{III} complexes with a tetragonally elongated octahedral geometry.[8]

Since the Mn^{III} ion is widely recognized as a "delicia of HFEPR spectroscopists",[8e] we performed multifrequency high-field EPR (HFEPR) measurements on a pellet of **1**. Mn^{III} again lived up to its fame, the complex producing exceptionally high-quality powder-pattern spectra from below 5 K to room temperature. Figures S5–S7 show the actual spectra at various frequencies and temperatures. Simulations of these spectra clearly confirm the negative sign of D, while the actual spin Hamiltonian parameters, including fourth-order zfs, were obtained from two-dimensional data arrays of resonance fields versus quantum energies at 10 and 280 K (Figure 2a and Figure S8). At 10 K the best fit for the $S = 2$ ground spin state was found with $D = -3.421(2)\ cm^{-1}$, $E = -0.152(2)\ cm^{-1}$ ($E/D = 0.044$), $B^4_0 = B^4_2 = 0$, $B^4_4 = 32(5) \times 10^{-4}\ cm^{-1}$, with very slightly anisotropic g factor ($g_1 = 1.994(2)$, $g_2 = 1.997(2)$, and $g_3 = 1.978(7)$). The negative sign of D (see the Supporting Information for further

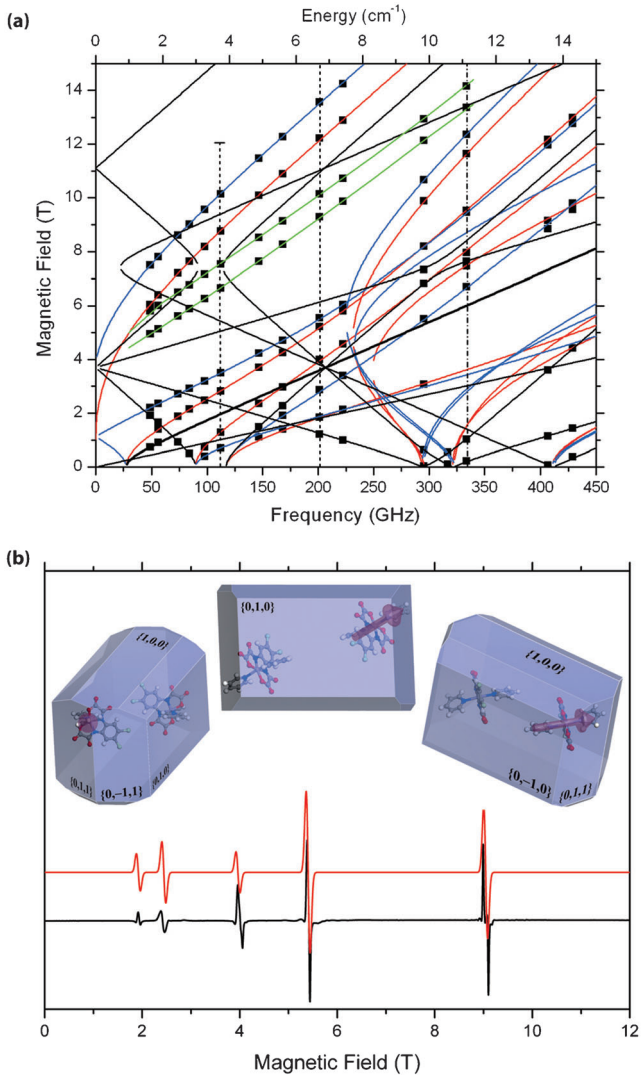

Figure 2. a) 2D map of HFEPR turning points in a pellet of **1** at 10 K. The squares are experimental resonances while the curves were simulated using best-fit spin Hamiltonian parameters (see text). Red curves: turning points with $B_0 \| x$, blue curves: $B_0 \| y$, black curves: $B_0 \| z$, and green curves: off-axis turning points. Only most prominent off-axis turning points are shown (several lesser turning points also show up at certain frequencies in the spectra). The vertical dashed lines represent the frequencies at which the spectra were recorded (see Supporting Information). b) Single-crystal HFEPR spectrum at 203.2 GHz and 10 K. The black trace: experiment; red trace: simulation. Several views of the relative orientation of two anionic mononuclear manganese(III) units into a single crystal of **1** are shown. The magenta arrow shows a rough orientation of the *z* axis of the zfs tensor. The {*h*,*k*,*l*} notation of the crystal faces are also indicated.

details) agrees perfectly well with the observed axial elongation of the coordination sphere of the Mn^{III} ion in **1**. The spin Hamiltonian parameters only slightly change with temperature; at 280 K they are: $D = -3.246(2)\ cm^{-1}$, $E = -0.115(1)\ cm^{-1}$ ($E/D = 0.035$), $B^4_0 = B^4_2 = 0$, $B^4_4 = 23(3) \times 10^{-4}\ cm^{-1}$ and $g = [2.001(1), 2.000(1), 1.990(3)]$.

We also performed single-crystal HFEPR experiments at 10 and 280 K (Figure 2b and Figure S9). The single crystal of **1** was oriented in such a way that the prominent {0,1,0} face was perpendicular to the magnetic field, that is, the crystallographic *b* axis was parallel to the field. In this orientation all four complexes present in the unit cell are magnetically equivalent, which results in one set of resonances only (Figure 2b). Simulations using the spin Hamiltonian parameters obtained from the pellet as described above are again of the highest quality (red traces in Figures 2b and S9), and show that the easy axes of the zfs tensor of individual complexes form the angles of $\pm 67°$ with the crystallographic *b* axis.

Complete active space (CAS) calculations were carried out to substantiate the influence of the structural distortions on the sign and magnitude of the axial magnetic anisotropy and rhombicity of **1** (see Supporting Information). The calculations show a moderately strong and negative *D* value ($D = -3.47\ cm^{-1}$) with a small rhombicity ($E/D = 0.014$), in agreement with the *zfs* of Mn^{III} complexes.[8f] Moreover, the *g* values calculated using the PBE functional ($g_1 = 2.003$, $g_2 = 2.004$, and $g_3 = 1.999$) are in agreement with the experimental ones independently derived from the least-squares fit of the experimental magnetic dc and HFEPR data. The not so good agreement in the *E*/*D* ratio is related to the usual difficulty to evaluate accurately the value of the *E* parameter. The *D* value of **1** calculated through the density functional (DFT) calculations using the PBE functional is slightly smaller in magnitude ($D = -2.53\ cm^{-1}$) than those provided by CAS calculations and obtained from experimental spectra, as previously reported in other mononuclear Mn^{III} complexes.[8]

CAS calculations allow identifying the nature and magnitude of the second order SOC contributions to the overall single-ion magnetic anisotropy of the high-spin d^4 Mn^{III} ion (Figure 3). The calculated axial magnetic anisotropy of the quintet ground state of **1** is mainly caused by the spin-orbit coupling ($D_{SOC} = -2.97\ cm^{-1}$). The spin–spin contribution ($D_{SS} = -0.50\ cm^{-1}$) is small but non-negligible. Due to the molecular geometry being not strictly D_{4h} or C_{2v}, the *z*-axis of the *D* tensor and the Jahn–Teller axis do not coincide (Figure S10). In good agreement with conclusions from the HFEPR study, the angle between the *z*-axis of the *D* tensor obtained from CAS calculations and the crystallographic *b* axis is 56.3 degrees. The spin–orbit contributions from other quintet excited states ($D_Q = -1.08\ cm^{-1}$) and from the mixing with triplet excited states ($D_T = -1.89\ cm^{-1}$) are both important and similar to those reported for precedent mononuclear high-spin Mn^{III} complexes.[8c–e] The relative energies of some of these excited states with respect to the $^5B_1$ ground state (Figure 3) from CAS calculations are 16270 ($^5A_1$), 21202 ($^5A_1$), 22311 ($^5B_2$), and 22704 cm^{-1} ($^5A_2$). Unfortunately, these energy values could not be compared with those provided from experimental electronic spectra in dichloromethane solution or in the solid state because of the presence of very intense charge transfer (CT) bands that mask the less intense d–d transitions for **1** (data not shown). However, these energy values are similar to those found previously in similar Mn^{III} complexes. Otherwise, the larger D_T value must be related to the fact that the low-lying ^3E and $^3A_1$ excited states obtained by the promotion of the single electron from the $d_{x^2-y^2}(\alpha)$ to the $t_{2g}(\beta)$ orbitals are very close in energy to the $^5B_1$ ground state ($\Delta = 18665$–$19790\ cm^{-1}$).[8c,d]

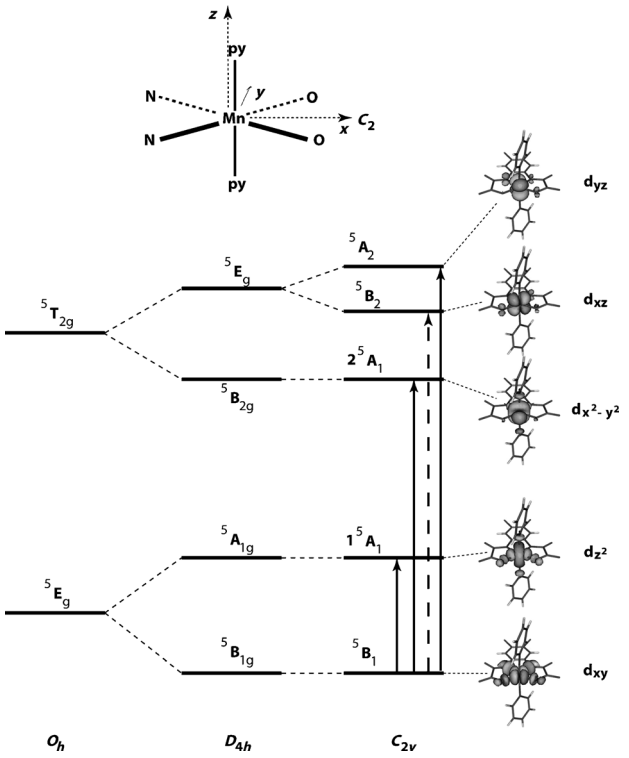

Figure 3. Splitting of the spectroscopic terms of the high-spin d^4 Mn^{III} ion of **1** when lowering the symmetry from O_h to C_{2v} with the elongation axis perpendicular to the C_2 axis. The labels refer to the symmetry elements shown at the top. The solid and dashed arrows show the allowed and forbidden d–d transitions, respectively. The empty orbitals are indicated for each state. The d_{z^2} and $d_{x^2-y^2}$ orbitals are mixed because they show the same symmetry.

The alternating current (ac) magnetic susceptibility of **1** in the form of the χ_M' and χ_M'' versus T plots (χ_M' and χ_M'' being the in-phase and out-of-phase ac magnetic susceptibilities per mononuclear unit) were then investigated. In zero dc magnetic field, no χ_M'' signals were observed even for the highest frequency used ($\nu = 10$ kHz; Figure S11). However, in an applied field of 1.0 kG, strong frequency-dependent maxima occur in both χ_M' and χ_M'' below 4.0 K (Figure 4 and Figure S12). The occurrence of slow magnetic relaxation effects in the presence of a moderately low dc magnetic field makes **1** the first example of field-induced SIM behavior in a mononuclear manganese(III) complex, the few other reported examples being mononuclear iron(I/II/III) and cobalt(II) species.[5] It implies that the superparamagnetic blocking is avoided because of the fast zero-field quantum tunneling relaxation of the magnetization.

The Cole–Cole plots of **1** in the temperature range of 3.0–4.0 K and at an applied field of 1.0 kG give almost perfect semicircles which can be fitted by the generalized Debye model (Figure S12).[10a] The calculated low values of the α parameter ($\alpha = 0.089$–0.216; Table S2) support a single relaxation process ($\alpha = 0$ for a Debye model), discarding a spin-glass behavior.[10b] Yet the overall increase of the α values from 0.089 ($T = 4.0$ K) to 0.216 ($T = 3.0$ K) evidences the occurrence of weak intermolecular interactions at these low temperatures.[11] On the other hand, the values of the relaxation time of **1**, which are calculated from the maximum of χ_M'' at a given frequency ($\tau = 1/2\pi\nu$), follow the Arrhenius law characteristic of a thermally activated mechanism ($\tau = \tau_0 \exp(E_a/k_B T)$; solid line in the inset of Figure 4). The calculated values of the pre-exponential factor and the activation energy ($\tau_0 = 1.24 \times 10^{-7}$ s and $E_a = 12.6$ cm^{-1}) are consistent with those previously reported for related iron(II) and cobalt(II) SIMs.[5] Moreover, the calculated E_a value for **1** compares reasonably well with those estimated from the fit of the magnetic dc and HFEPR data ($E_a = -4D = 13.2$ and 13.7 cm^{-1}, respectively).

To further confirm the unique field-induced slow magnetic relaxation behavior of **1**, additional dc magnetization measurements at very low temperatures were performed on single crystals using a micro-SQUID (see the Supporting Information). The observed hysteresis loops of **1** are strongly temperature- and field sweep rate-dependent (Figure 5 and Figure S13). Moreover, they show a characteristic butterfly shape, as found in related mononuclear iron(I/II/III) and cobalt(II) complexes with a similar field-induced SIM behavior.[5] In fact, the quantum tunneling effects lead to very closed hysteresis loops at a zero dc field, in agreement with the ac magnetic susceptibility measurements. In addition, the

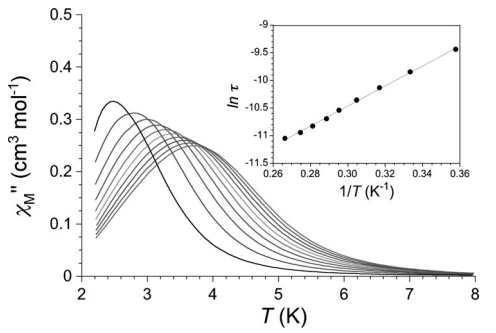

Figure 4. Temperature dependence of χ_M'' of **1** in a dc applied static field of 1.0 kG and in a ± 4.0 G oscillating field at frequencies in the range of 1–10 kHz. Inset: the Arrhenius plot in the high-temperature region. The solid line is the best fit-curve (see text).

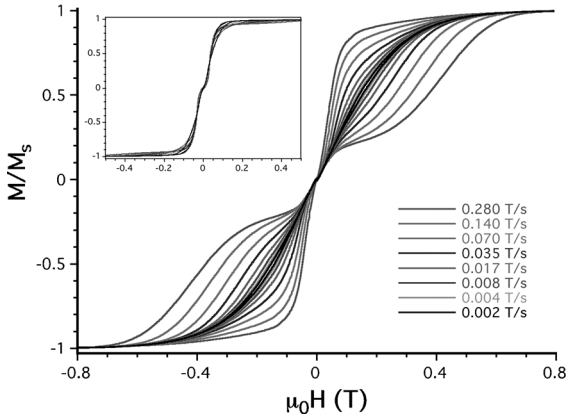

Figure 5. Field dependence of the normalized magnetization of **1** at 0.5 K with varying field sweep rates in the range of 2–280 mTs^{-1}. Inset: hysteresis loops at a lower temperature of 0.03 K.

hysteresis practically disappears at the lowest available temperature of 30 mK, owing to the fast tunneling of the magnetization of the ground state (inset of Figure 5).

In conclusion, we report the first example of a mononuclear manganese(III) complex which behaves as a SIM, the few other reported examples of SIMs based on first-row transition-metal ions are for mononuclear iron(I/II/III) and cobalt(II) complexes. In this respect, it is surprising that no report on a manganese-based SIM has been appeared to date,[12] given the importance of manganese in the birth and history of molecular nanomagnets. The large Jahn–Teller distortion of the octahedral environment of the Mn^{III} ion in **1**, which obeys the strong electron donating nature (basicity) of the planar tetradentate opbaCl_2 chelating ligand, is responsible for the moderately large and negative value of the axial magnetic anisotropy ($D < 0$) and the non-negligible rhombicity ($E/D \neq 0$), as confirmed by magnetization and HFEPR spectroscopic measurements and further supported by CAS calculations. Current efforts are devoted to investigating the influence of the electronic and steric effects of the ligand substituents so as to give a new series of oxamato-containing mononuclear manganese(III) complexes with axially elongated, octahedral geometries, and large negative D values as a new class of manganese-based SIMs.

Received: September 13, 2013
Published online: November 19, 2013

Keywords: CAS calculations · EPR spectroscopy · magnetic properties · manganese · oxamato ligands

[1] D. Gatteschi, R. Sessoli, J. Villain, *Molecular Nanomagnets*, Oxford University Press, Oxford, **2006**.

[2] a) M. N. Leuenberger, N. Loss, *Nature* **2001**, *410*, 789; b) M. Affronte, F. Troiani, A. Ghirri, A. Candini, M. Evangelisti, V. Corradini, S. Carretta, P. Santini, G. Amoretti, F. Tuna, G. Timco, R. E. P. Winpenny, *J. Phys. D* **2007**, *40*, 2999; c) L. Bogani, W. Wernsdorfer, *Nat. Mater.* **2008**, *7*, 179.

[3] a) R. Sessoli, D. Gatteschi, A. Caneschi, M. A. Novak, *Nature* **1993**, *365*, 141; b) J. R. Friedman, M. P. Sarachik, J. Tejada, R. Ziolo, *Phys. Rev. Lett.* **1996**, *76*, 3830.

[4] a) A. J. Tasiopoulos, A. Vinslava, W. Wernsdorfer, K. A. Abboud, G. Christou, *Angew. Chem.* **2004**, *116*, 2169; *Angew. Chem. Int. Ed.* **2004**, *43*, 2117; b) Q. Wu, Y.-G. Li, Y. H. Wang, R. Clérac, Y. Lu, E.-B. Wang, *Chem. Commun.* **2009**, 5743.

[5] a) D. E. Freedman, W. H. Harman, T. D. Harris, G. J. Long, C. J. Chang, J. R. Long, *J. Am. Chem. Soc.* **2010**, *132*, 1224; b) W. H. Harman, T. D. Harris, D. E. Freedman, H. Fong, A. Chang, J. D. Rinehart, A. Ozarowski, M. T. Sougrati, F. Grandjean, G. J. Long, J. R. Long, C. J. Chang, *J. Am. Chem. Soc.* **2010**, *132*, 18115; c) D. Weismann, Y. Sun, Y. Lan, G. Wolmershauser, A. K. Powell, H. Sitzmann, *Chem. Eur. J.* **2011**, *17*, 4700; d) P.-H. Lin, N. C. Smythe, S. I. Gorelsky, S. Maguire, N. J. Henson, I. Korobkov, B. L. Scott, J. C. Gordon, R. T. Baker, M. Murugesu, *J. Am. Chem. Soc.* **2011**, *133*, 15806; e) T. Jurca, A. Farghal, P.-H. Lin, I. Korobkov, M. Murugesu, D. S. Richardson, *J. Am. Chem. Soc.* **2011**, *133*, 15814; f) J. M. Zadrozny, J. R. Long, *J. Am. Chem. Soc.* **2011**, *133*, 20732; g) J. M. Zadrozny, J. Liu, N. A. Piro, C. J. Chang, S. Hill, J. R. Long, *Chem. Commun.* **2012**, *48*, 3927; h) J. Vallejo, I. Castro, R. Ruiz-García, J. Cano, M. Julve, F. Lloret, G. D. Munno, W. Wernsdorfer, E. Pardo, *J. Am. Chem. Soc.* **2012**, *134*, 15704; i) S. Mossin, B.-L. Tran, D. Adhikari, M. Pink, F. W. Heinemann, J. Sutter, R. K. Szilagyi, K. Meyer, D. J. Mindiola, *J. Am. Chem. Soc.* **2012**, *134*, 13651; j) E. Colacio, J. Ruiz, E. Ruiz, E. Cremades, J. Krzystek, S. Carreta, J. Cano, T. Guidi, W. Wernsdorfer, E. K. Brechin, *Angew. Chem.* **2013**, *125*, 9300; *Angew. Chem. Int. Ed.* **2013**, *52*, 9130; k) J. M. Zadrozny, D. J. Xhiao, M. Atanasov, G. J. Long, F. Grandjean, F. Neese, J. R. Long, *Nat. Chem.* **2013**, *5*, 577.

[6] S. Romain, C. Duboc, F. Neese, E. Rivière, L. R. Hanton, A. G. Blackman, C. Philouze, J. C. Lepêtre, A. Deronzier, M. N. Collomb, *Chem. Eur. J.* **2009**, *15*, 980.

[7] a) M. Fettouhi, L. Ouahab, A. Boukhari, O. Cador, C. Mathonière, O. Kahn, *Inorg. Chem.* **1996**, *35*, 4932; b) S. Barroso, G. Blay, I. Fernández, J. R. Pedro, R. Ruiz-García, E. Pardo, F. Lloret, M. C. Muñoz, *J. Mol. Catal. A* **2006**, *243*, 214.

[8] a) D. P. Goldberg, J. Telser, J. Krzystek, A. Garrido-Montalban, L.-C. Brunel, A. G. M. Barrett, B. M. Hoffman, *J. Am. Chem. Soc.* **1997**, *119*, 8722; b) J. Krzystek, J. Telser, B. M. Hoffman, L.-C. Brunel, S. Licoccia, *J. Am. Chem. Soc.* **2001**, *123*, 7890; c) J. Krzystek, J. Telser, L. A. Pardi, D. P. Goldberg, B. M. Hoffman, L. C. Brunel, *Inorg. Chem.* **1999**, *38*, 6121; d) B. Albela, R. Carina, C. Policar, S. Poussereau, J. Cano, J. Guilhem, L. Tchertanov, G. Blondin, M. Delroisse, J. J. Girerd, *Inorg. Chem.* **2005**, *44*, 6959; e) I. Krivokapic, C. Noble, S. Klitgaard, P. L. W. Tregenna-Piggott, H. Weihe, A.-L. Barra, *Angew. Chem.* **2005**, *117*, 3679; *Angew. Chem. Int. Ed.* **2005**, *44*, 3613; f) C. Duboc, D. Ganyushin, K. Sivalingam, M. N. Collomb, F. Neese, *J. Phys. Chem. A* **2010**, *114*, 10750.

[9] J. Cano, VPMAG, Univerity of Valencia, Spain, **2001**.

[10] a) K. S. Cole, R. H. Cole, *J. Chem. Soc.* **1941**, *9*, 341; b) J. A. Mydosh, *Spin Glasses: An Experimental Introduction*, Taylor & Francis, London, **1993**.

[11] L. M. Toma, C. Ruiz-Pérez, J. Pasán, W. Wernsdorfer, F. Lloret, M. Julve, *J. Am. Chem. Soc.* **2012**, *134*, 15265.

[12] During the preparation of this manuscript, a Communication from Ishikawa et al. has appeared that reports on slow relaxation of the magnetization in a heterodinuclear low-spin cobalt(III)/high-spin manganese(III) complex (see R. Ishikawa, R. Miyamoto, H. Nojiri, B. K. Breedlove, M. Yamashita, *Inorg. Chem.* **2013**, *52*, 8300. However, no direct evidence of SIM behavior has been given therein, asides of the occurrence of incipient out-of-phase ac magnetic susceptibility signals at low temperatures which can be indicative of slow magnetic relaxation effects (but also of a long-range magnetic ordering). Note added in proof (Sept. 5, 2013): Recently, we have been informed of another report of a mononuclear six-coordinated manganese(III) complex showing characteristics of a SIM by P. Kyritsis, Y. Sanakis et al. unpublished results.

[13] CCDC 953476, contain the supplementary crystallographic data for this paper. These data can be obtained free of charge from The Cambridge Crystallographic Data Centre via www.ccdc.cam.ac.uk/data_request/cif.

